ENSTA Bretagne · Ifremer
15ÈMES JOURNÉES DE L'HYDRODYNAMIQUE
22 - 24 novembre 2016 - Brest

Validation of a Navier-Stokes model to study flip-through impacts on a vertical breakwater

Validation d'un modèle Navier-Stokes pour l'étude des impacts du type flip-through sur un brise-lames vertical

M. Martin-Medina[(1)], **S. Abadie**[(1)], and **D. Morichon**[(1)]

[(1)]SIAME EA 4581, Université de Pau et des Pays de l'Adour, Anglet, France

Summary :

Two validations of the Navier-Stokes VOF model THETIS are presented in this study: the uplift pressures on a rubble mound due to wave impacts and flip-through impacts on a vertical wall. The first validation case allows us to show the overall ability of the model to reproduce uplift pressure due to wave impacts inside a porous medium. A sudden pressure increase was observed due to a strong compression of enclosed air in the rubble mound. Then, the flip-through phenomenon is modelled using the THETIS model. These results are compared with other numerical data computed with a potential model. The Navier-Stokes simulations underestimate pressures along the wall. The wave interface is modified by the presence of air, which is not considered in the potential model, and this seems to be enough to generate such pressure differences.

Résumé :

Deux cas de validation du modèle THETIS (Navier-Stokes VOF) sont présentés dans cette étude: les pressions de soulèvement sur un talus poreux due à l'impact des vagues et des impacts flip-through sur un mur vertical. Le premier cas de validation nous permet de montrer la capacité du modèle à reproduire variations de pression due à l'impact d'une vague dans un milieu poreux. Une augmentation soudaine de la pression a été observée en raison d'une forte compression de l'air piégé dans le talus poreux. Ensuite, le phénomène flip-through est modélisé avec THETIS. Les résultats sont comparés avec d'autres données numériques calculées avec un modèle potentiel. Les simulations de Navier-Stokes sous-estiment les pressions au long du mur. L'interface de la vague est légèrement modifiée par la présence d'air, qui n'est pas pris en compte dans le modèle de potentiel, et cela semble être suffisant pour générer ces différences de pression.

1 Introduction

A vertical breakwater is usually composed of a concrete caisson placed on top of a rubble mound. The advantages of such structure is to require less material compared to rubble mound breakwater to reach a high elevation. However, while rubble mound breakwater damages under storm waves attack are progressive, vertical breakwater collapse may be sudden and brutal. This also due to the fact that the caisson presents a flat face to the wave attack which favour large impulsive pressure occurrence.

Several methods have been proposed to calculate the pressure distribution of the design wave to study the stability of the structure (Goda [8], Takahashi et al. [22] Takahashi et al. [23], Oumeraci et al. [18], Cuomo et al. [2]). These studies were focused on the practical design problem and not really on the processes acting to destabilize the structure. In this context, numerical models can be a valuable tool for identifying the important parameters in this problem.

So far, most published numerical works were more focused on the validation of the model for practical purpose involving several wave (regular or irregular) than on the impact process at the wave scale. Hsu et al. [14] presented the first Navier-Stokes VOF results for wave interaction with a composite breakwater including a rubble mound. Garcia et al. [7], Losada et al. [17], Lara et al. [16] studied the turbulent flow generated by regular and irregular waves within and outside a porous breakwater using the same kind of models. Guanche et al. [9] performed in-depth validation study of a Navier-Stokes model for the prediction irregular wave load on a vertical breakwater. del Jesus et al. [3], Lara et al. [15], Higuera et al. [11] and Higuera et al. [12] continued this validation process in 3D.

The present work also uses a Navier-Stokes model to study wave impact on a vertical breakwater at the wave scale. The focus is on the specific flip-through impact which is known to generate the highest pressure on the structure face (Peregrine [20]). The overall objective of this work is to detail the processes and further better understand the structure behaviour under very violent impacts. As a first step, in this paper, we present the validation of the model for the flip through impact and the uplift pressure pressure generated in the rubble mound.

2 Method

2.1 The model

The numerical model THETIS solves the Navier–Stokes (NS) equations and uses a Volume of Fluid Technique (VOF) method to capture the interface evolution. The flow considered incompressible is composed of two immiscible phases: water and air. The continuity of fluid velocity is assumed through the interface and the surface tension effects are neglected. The THETIS code was extended in order to model multiphase flows inside porous mediums in Desombre et al. [4]. The flow simulation in the porous medium is based on the Forchheimer equation which relates the hydraulic gradient I and the Darcy velocity $\boldsymbol{\nu}$.

$$I = a_k \boldsymbol{\nu} + b_k \|\boldsymbol{\nu}\| \boldsymbol{\nu} \tag{1}$$

This velocity is the volume-averaged velocity over the cells mesh which is linked to the internal pore velocity V by the Dupuit relationship $\boldsymbol{\nu} = V\phi$. The linear and quadratic drag coefficients are related to the intrinsic permeability and to the fluid density and viscosity by the respective relations:

$$a_k = \frac{\mu}{\rho g k} \qquad and \qquad b_k = \frac{C_F}{g\sqrt{k}} \tag{2}$$

The Forchheimer equation (1) is an extension of the Darcy equation. The quadratic drag term extends the Darcy law to higher Reynolds flow regime, so called the Forchheimer regime. Integrating the Darcy-Brinkman-Forchheimer formulation, the system of equations solved by THETIS is the following:

$$\nabla \cdot \boldsymbol{\nu} = 0 \tag{3}$$

$$\rho\left(\frac{1}{\phi}\frac{\partial \boldsymbol{\nu}}{\partial t} + \frac{\boldsymbol{\nu}}{\phi} \cdot \nabla \frac{\boldsymbol{\nu}}{\phi}\right) + \nabla p - \mu_{eff} \nabla^2 \boldsymbol{\nu} + \frac{\mu}{k} + \frac{\rho C_F}{\sqrt{k}} = \rho \mathbf{g} \tag{4}$$

where, ρ is the fluid density, $\mu_{eff} = \dfrac{\mu}{\phi}$ the effective viscosity and C_F the Forchheimer coefficient.

Outside of the porous medium, the porosity is $\phi = 1$ and the intrinsic permeability is set to $k = \infty$. The equation (4) is therefore transformed to the classical NS equation. Inside the porous medium, the porosity and the permeability are low and Darcy and Forchheimer terms allow to balance the hydraulic gradient Thus, surface and subsurface flows can be simultaneously solved while ensuring continuity at the boundary.

This system of equations is discretized on a fixed Cartesian grid using a finite volume formulation. Following Patankar [19], the finite volume formulation is solved using a staggered mesh known as the Marker And Cells (MAC) method from Harlow et al. [10]. The coupling between velocity and pressure is solved using the augmented Lagrangian method (Fortin and Glowinski [6]). This is a minimization method under the constraint of the continuity equation, where the pressure which is decoupled from the velocity, appears as a Lagrange multiplier.

A Volume of Fluid (VOF) method (Hirt and Nichols [13]) that describes the volume fraction occupied by one of the fluids (i.e. water) in a cell, the Piecewise Linear Interface Calculation (PLIC) method, is employed in these simulations. This Eulerian/Lagrangian method allows to keep the discontinuous nature of the interface between water and air using the Lagrangian character of the transport method. The stability of the PLIC method is ensured by imposing that the volume fraction does not move more than half of a cell during a time step (Abadie et al. [1]). To reduce problems related to the continuity of the interface during violent impacts, a smoothing algorithm (SVOF) can be added to the PLIC method. This algorithm allows to smooth the volume fraction function by introducing a controlled diffusion zone around the interface.

2.2 Test cases

2.2.1 Solitary wave breaking on a vertical breakwater

Numerical results are compared to laboratory experiments carried out in the Coastal Wave, Current and Tsunami Flume (COCOTSU) at the IH Cantabria in the framework of the ASTARTE european project on tsunami risk. The aim of these experiments is to measure the complex flow generated by a solitary wave interacting with a rubble mound breakwater. The model set-up is represented in Figure 1. The main characteristics of the experiment are summarized in table 1. Solitary waves of several heights are tested during the experiments, but we only keep a wave of 0.20 cm to validate the numerical model. The displacement of the crown is not permitted and its material is considered non permeable. The rubble mound is composed by a permeable core covered by an outer armor and an inner armor. This analysis is focused on the pressure inside the porous medium as the wave impact on the screen does not correspond to the kind of wave impact of our interest: the flip-through on a vertical composite breakwater.

A filter layer is placed between the core and outer armor layer. The numerical domain is discretized in 462000 elements by using an irregular mesh with a minimal size of $0.005m$ in the impact area. Slip conditions are imposed along the model boundaries. For the numerical simulations, the porosity and intrinsic permeability of the rubble mound are fixed for each studied case in table 2. The intrinsic permeability is estimated by the Kozeny-Carman formulae giving approached values. The solitary waves are modelled using the third order solution given in Fenton [5].

Variable	Units	Model
Water depth	m	0.4
Design wave height H_{50}	m	0.32
Size outer armor stones (D_5 - D_{95})	m	$0.055 - 0.067$
Outer armor layer thickness ($2D_{50}$)	m	0.123
Size filter-inner stones (D_5 - D_{95})	m	$0.027 - 0.042$
Filter-inner thickness ($2D_{50}$)	m	0.072
Core stones size (D_{10} - D_{95})	m	$0.011 - 0.052$

Table 1 – Model characteristics.

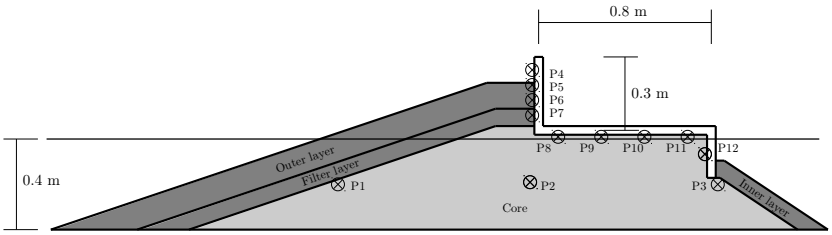

Figure 1 – Breakwater characteristics and pressure gauges location

	Porosity	Outer permeability $[m^2]$	Filter-inner permeability $[m^2]$	Core permeability $[m^2]$
Cas 1	0.5	10^{-4}	10^{-5}	10^{-5}
Cas 2	0.4	10^{-4}	10^{-5}	10^{-5}
Cas 3	0.5	10^{-5}	10^{-6}	10^{-6}
Cas 4	0.5	10^{-5}	10^{-5}	10^{-5}

Table 2 – Characteristics of the studied cases for the flip-through impact.

2.2.2 Flip through impact

THETIS is also validated in this paper for flip-though impacts. The reference case is the numerical simulations of Scolan [21] which uses the potential theory to study several flip-through impacts. The effect of air and the surface tension are neglected with this model. The simulations start from the following initial free surface deformation in a rectangular tank without varying the bathymetry:

$$y = h + A\tanh(R(x - L/2)), \qquad 0 < x < L \tag{5}$$

where L is the length of the rectangular tank, h is the water depth, A is the amplitude and R controls the slope of the height amplitude. Figure 2 shows the numerical set-up of the studied case in this work. Free slip conditions are imposed in the Navier-Stokes model. The characteristics of the simulations are summarized in table 3. The effect of air during the impact is analysed by modifying the density of air.

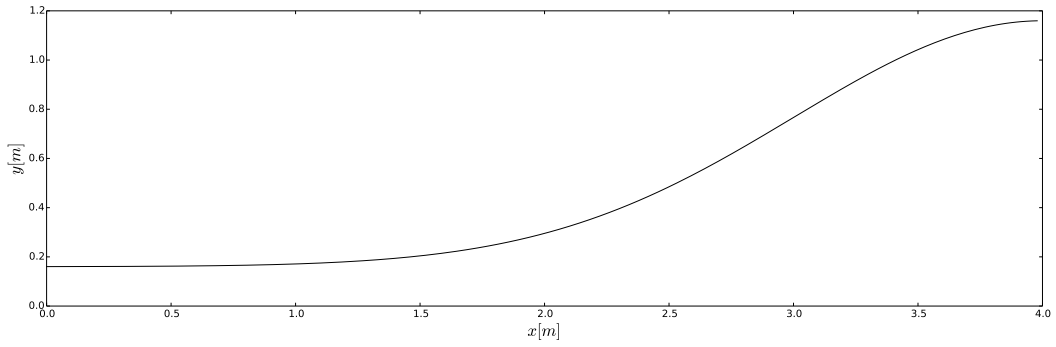

Figure 2 – Numerical set-up of the flip-through impact case. $A = 1$m, $h = 0.16$m, $R = 0.5$m and $L = 4$m.

	Mesh	Minimal mesh size [m]	ρ_{air} [Kg/m^3]
Cas 1	800×250	0.005	1.1768
Cas 2	1600×500	0.0025	1.1768
Cas 3	800×800	0.001	1.1768
Cas 4	800×800	0.001	1.1768×10^{-2}
Cas 5	800×800	0.001	1.1768×10^{-8}

Table 3 – Characteristics of the studied cases for the flip-through impact.

3 Results

3.1 Solitary wave breaking on a rubble mound breakwater

The aim of this section is to show the variations in terms of pressure due to porosity and permeability changes. Figure 3 illustrates the pressure evolution on time for two different porosities of the rubble mound. Overall, very similar pressure values are obtained for the two cases being in a good agreement with the laboratory experiments. We observe the existence of a remarkable pressure peak that does not appear in the experimental data. We analyse the causes of this peak pressure in the last part of this section.

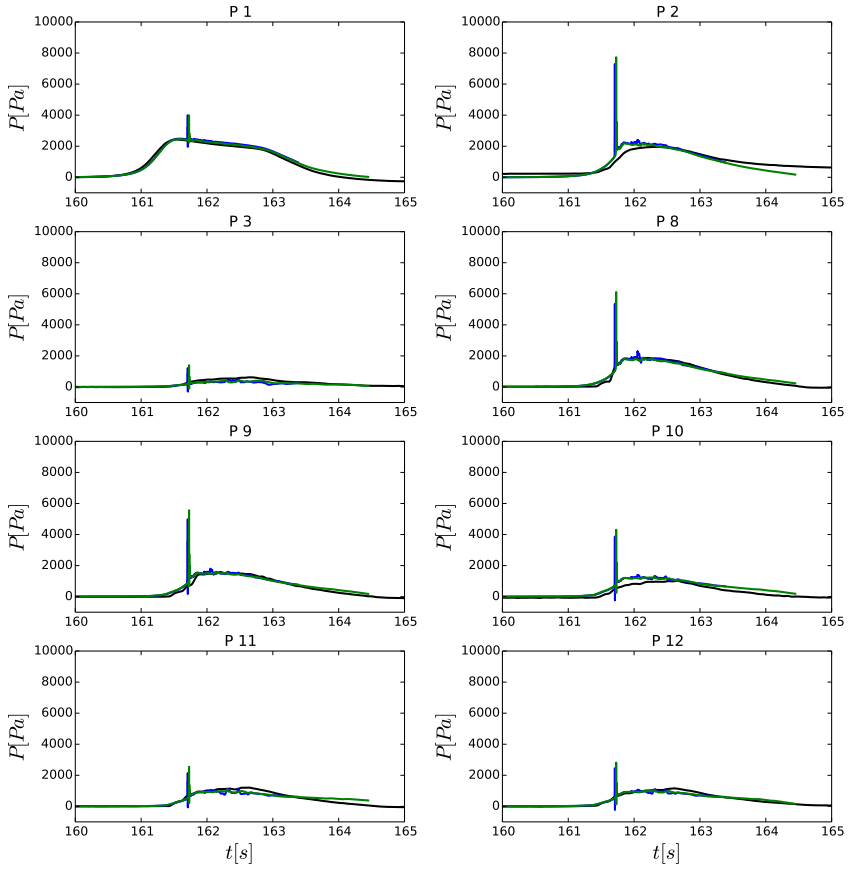

Figure 3 – Pressure evolution on time inside the porous medium. Experimental data (–), case 1 (–) and case 2 (–).

Figure 4 compares the time evolution of the pressures due to solitary wave impacts on the rubble mounds with different permeability values. The mentioned pressure peak is present for the three studied cases. However, case 1 gives the best results after the peak. Case 3, which has the lowest permeability values, presents pressure fluctuations and the computation stopped before the end of the wave impact (t=162.2s) due to significant numerical instabilities. The case with constant permeability (case 4) gives similar results to case 1 but presenting slight pressure undulations that are not observed in the experimental data.

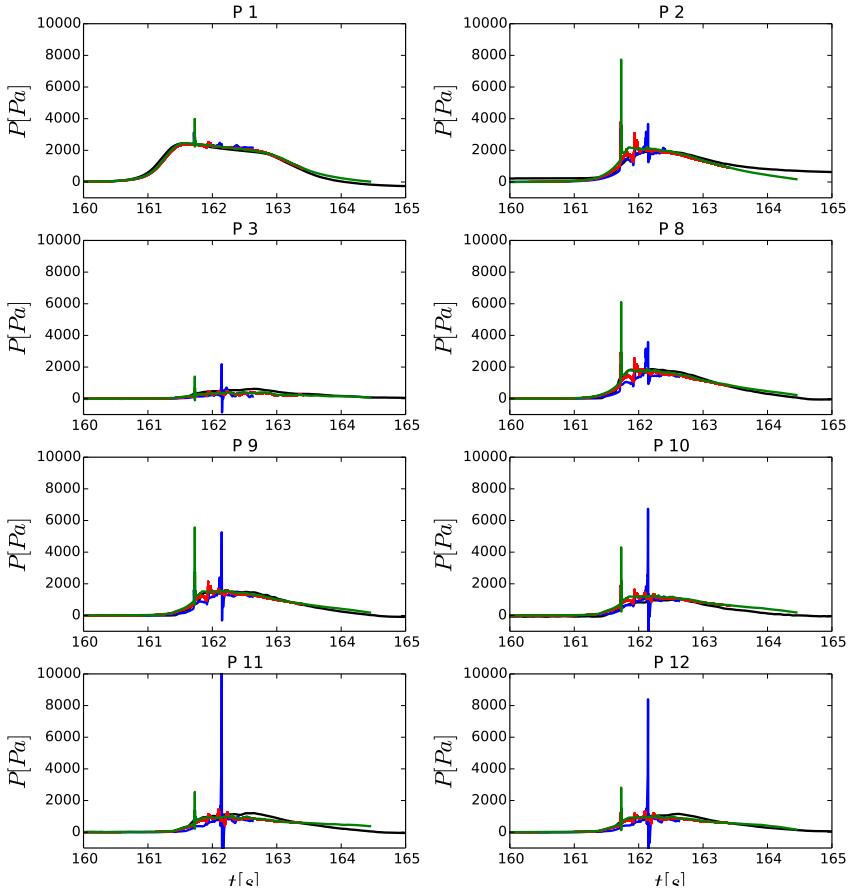

Figure 4 – Pressure evolution on time inside the porous medium. Experimental data (–), case 1 (–), case 3 (–) and case 4 (–).

Figure 5 shows a more detailed view of the pressure peak time evolution in sensors P1, P2 and P3 located in the core. The only difference between the two cases analysed resides on the outer layer permeability (10^{-4} for case 1 and 10^{-5} for case 4). Figure 6 illustrates the wave interface, velocity field and pressures within the breakwater. As we can see in these figures, the pressure peak appears just milliseconds before the solitary wave crest meets the screen. This sharp pressure increase is preceded by a violent air flow going out the porous medium due to the wave front penetration inside the rubble mound. The pressure peak appears when the wave front outside the rubble mound is about to meet the screen. At this time, air is partially enclosed in the rubble mound and it is compressed by the wave front which causes a general and sudden pressure augmentation. As the model is incompressible, once the air is evacuated, the pressure goes back to normal values. The air pocket shape seems to play an important role in the pressure peak value. Therefore, as case 2 presents the more permeable outer layer, the wave front moves faster than in case 4 and this leads to a small air pocket which gives the largest pressure values. The pressure peak undulations observed in figure 5 may be related to the effect of the enclosed air associated to numerical pseudo-compressibility. Tests taking into account air compressibility were carried out but pressure peaks were also observed associated to more significant undulations.

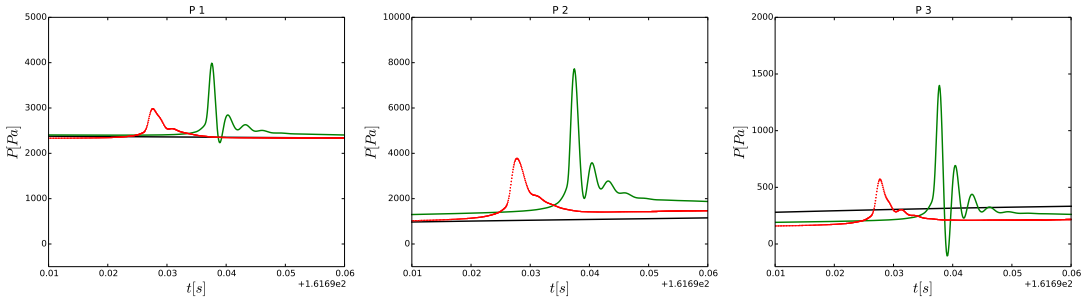

Figure 5 – Pressure peak recorded in the core rubble mound. Experimental data (–), case 2 (–) and case 4 (–).

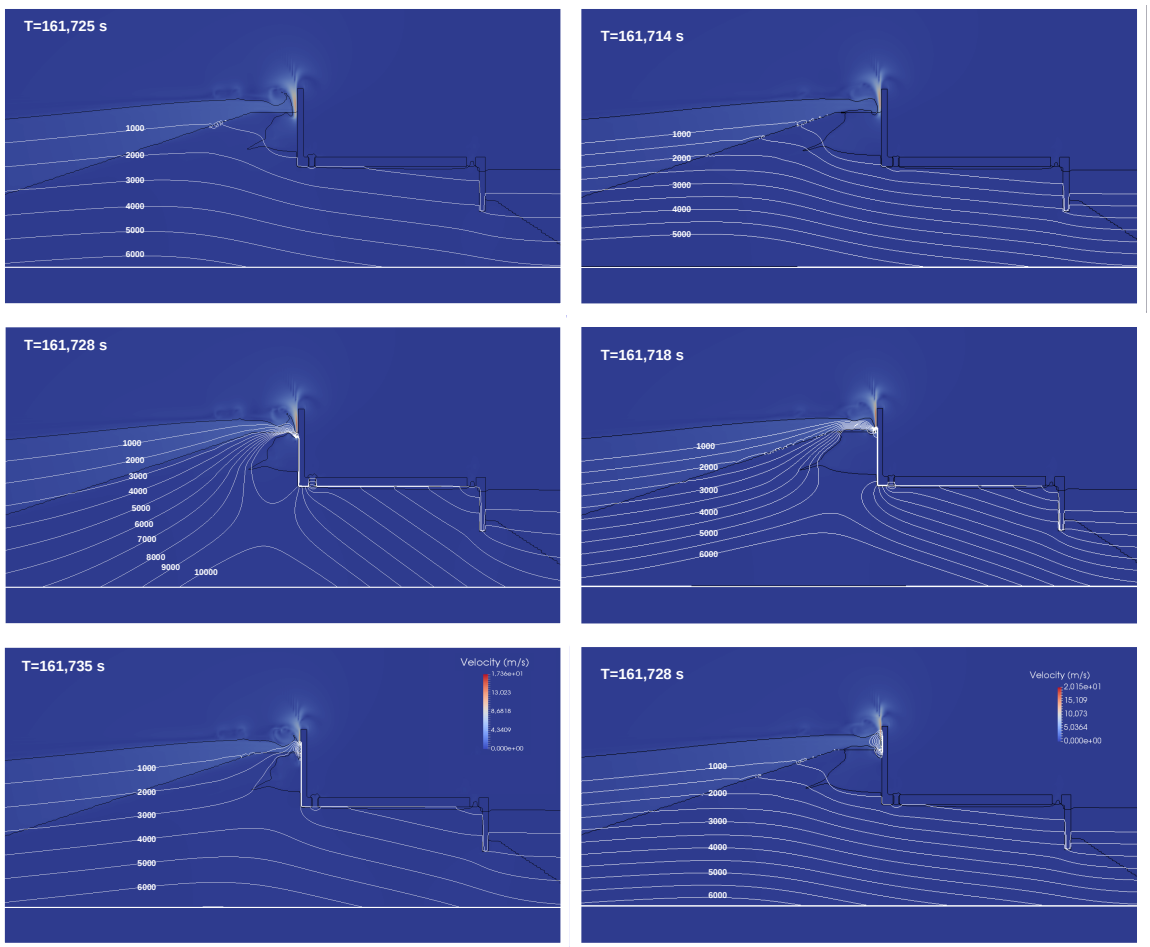

Figure 6 – Snapshot of the pressure peak (Pa) increase for the case 2 (left) and case 4 (right).

3.2 Flip through impact

3.2.1 Influence of the mesh size

Figure 7 presents the water/air interface depending on the mesh cell size. We can first observe instabilities and drops that appear for the coarsest mesh. These instabilities become undulations in the wave crest with the finest mesh. Overall, the navier-Stokes simulations are not able to reproduce the steep wave face obtained with the potential model. Figure 8 shows the pressure distributions for the three studied meshes. Very similar pressure values are obtained for the three cases. However, these results and the pressure distributions given by Scolan [21] are not in a good agreement. This is directly linked to the different wave steepnesses obtained with the two numerical model. These differences may be related to the air influence which is investigated in the further section.

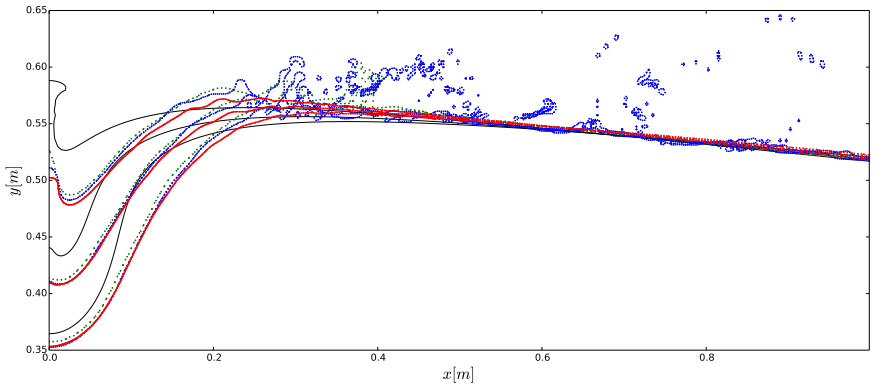

Figure 7 – Interface evolution at impact. Data from Scolan (–), case 1 (–), case 2 (–) and case 3 (–). $t = 0.97$ s, $t = 0.98$ s, $t = 0.99$ s.

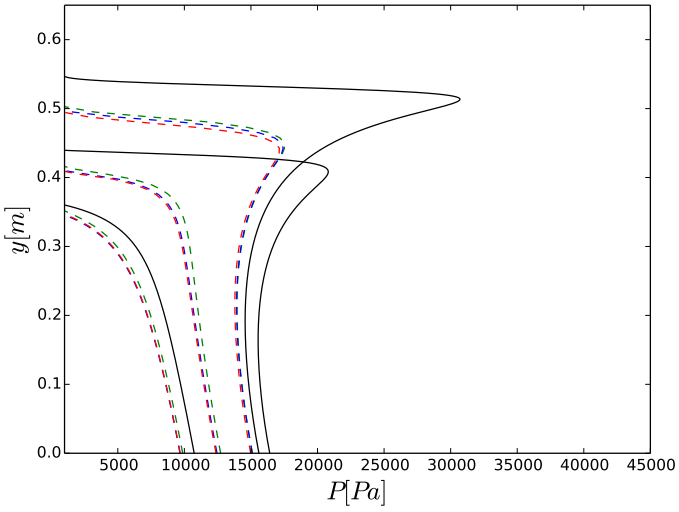

Figure 8 – Pressure distribution along the wall at impact. Data from Scolan (–), case 1 (- -), case 2 (- -) and case 3 (- -). $t = 0.97$ s, $t = 0.98$ s, $t = 0.99$ s.

3.2.2 Air effect

The air influence on the interface during flip-through impacts is analysed in this section. For this purpose, we artificially modify the air density in the Navier-Stokes model. Hence, we compare the case with the real air density with two cases composed of a less dense "air" ($\rho_{air} \times 10^{-2}$ and $\rho_{air} \times 10^{-8}$). The later value being

our limit case as simulations performed with even less dense air lead to the same results. Figure 9 illustrates the interface of each considered case at impact. The undulations mentioned before do not appear for the case with the lightest air (case 5). We observe than the water seems to be stopped by the effect of air. Therefore, the interfaces obtained with the cases 3 and 4 present a delay compared to Scolan's results. This is less flagrant for case 5. It is important to highlight that the effect of air generally becomes more significant while the fluid velocity rise along the wall and so the interface differences increase from the beginning to the end of the impact. Figure 10 compares pressure distributions for the three studied cases. We can first observe that there is a direct link between pressures and the interface shape at impact. Hence, case 5 generates the highest pressure on the wall which has to be related to the steepest wave face at impact. However, the Navier-Stokes model is not able to reproduce the same conditions as the potential model and slight different pressure values are still obtained for each model.

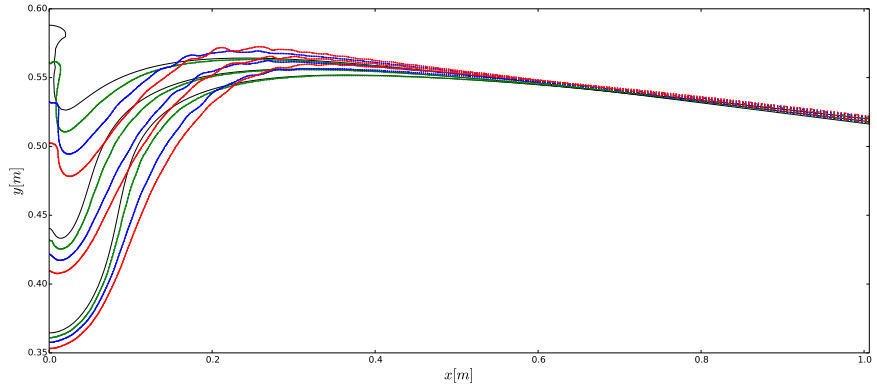

Figure 9 – Interface evolution at impact. Data from Scolan (–), $\rho_{air} \times 10^{-8}$ (–), $\rho_{air} \times 10^{-2}$ (–) and ρ_{air} (–). $t = 0.97$ s, $t = 0.98$ s, $t = 0.99$ s.

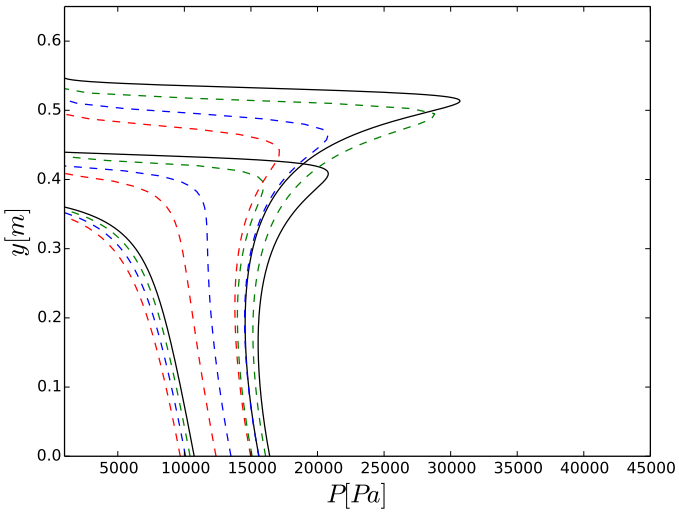

Figure 10 – Pressure distribution along the wall at impact. Data from Scolan (–), $\rho_{air} \times 10^{-8}$ (- -), $\rho_{air} \times 10^{-2}$ (- -) and ρ_{air} (- -). $t = 0.97$ s, $t = 0.98$ s, $t = 0.99$ s.

4 Conclusions

THETIS was validated for wave impacts into a porous composite breakwater and flip-through impacts in this paper. Laboratory experiments have been used for the first validation. A numerical study of the flip-through

phenomenon has been considered for the second validation due to the lack of detailed experimental studies. The following main conclusions can be drawn:

- Effect of porosity and permeability changes during wave impacts on the porous medium: changing the porosity in the armor layers or in the core does not seem to play an important role on the pressure field inside porous mediums, whereas permeability changes in the armor layers and core generate significant pressure variations in the beginning of the wave impact.
- Sharp pressure peak due to wave impacts on a porous rubble mound: a high and fast pressure increase was observed for all the studied cases which does not exist in the experiment. It has been shown that these pressure peaks are caused by a strong compression of enclosed air inside the porous medium. The pressure peak value is directly linked to the permeability of the outer layer.
- Influence of the mesh size on the flip-through phenomenon: interface instabilities and drops appear with coarse mesh.
- The shape seems to be strongly influence by the surrounding air: Comparing to the data presented in Scolan [21], the wave seems to be stopped by the air. This effect is increased at the time of impact. Reducing the air density, the Navier-Stokes results are in a better agreement with the velocity potential model.

This validation will serve as a basis for a further numerical experiment consisting of studying the pressures generated by various flip-though impacts and investigating the caisson stability under these forcings.

Acknowledgement

This work was funded by the PIA RSNR French program Tsunamis in the Atlantic and the English ChaNnel (Grant No.: ANR-11-RSNR-00023-01) and by the FP7 EU research program ASTARTE (Grant No.:603839). The authors would like to thank Dr. Yves-Marie Scolan for assistance with the flip-through phenomenon and acknowledge IH Cantabria for the experimental data of solitary waves interacting with the rubble mound breakwater.

References

[1] S Abadie, J Caltagirone, and P Watremez. Splash-up generation in a plunging breaker. *Comptes Rendus de l'Academie des Sciences Series IIB Mechanics Physics Astronomy*, 326(9):553–559, 1998.

[2] Giovanni Cuomo, William Allsop, Tom Bruce, and Jonathan Pearson. Breaking wave loads at vertical seawalls and breakwaters. *Coastal Engineering*, 57(4):424–439, 2010.

[3] Manuel del Jesus, Javier L Lara, and Inigo J Losada. Three-dimensional interaction of waves and porous coastal structures: Part i: Numerical model formulation. *Coastal Engineering*, 64:57–72, 2012.

[4] Jonathan Desombre, Denis Morichon, and Mathieu Mory. Simultaneous surface and subsurface air and water flows modelling in the swash zone. *Coastal Engineering Proceedings*, 1(33):56, 2012.

[5] John Fenton. A ninth-order solution for the solitary wave. *Journal of Fluid Mechanics*, 53(02):257–271, May 1972. ISSN 1469-7645. doi: 10.1017/S002211207200014X. URL `http://journals.cambridge.org/article`$_S$002211207200014X.

[6] Ml Fortin and R Glowinski. *Méthodes de lagrangien augmenté: applications à la résolution numérique de problèmes aux limites*. Dunod, 1982.

[7] N Garcia, JL Lara, and IJ Losada. 2-d numerical analysis of near-field flow at low-crested permeable breakwaters. *Coastal Engineering*, 51(10):991–1020, 2004.

[8] Yoshimi Goda. New wave pressure formulae for composite breakwaters. *Coastal Engineering Proceedings*, 1(14), 1974.

[9] Raul Guanche, Inigo J Losada, and Javier L Lara. Numerical analysis of wave loads for coastal structure stability. *Coastal Engineering*, 56(5):543–558, 2009.

[10] F H Harlow, J E Welch, et al. Numerical calculation of time-dependent viscous incompressible flow of fluid with free surface. *Physics of fluids*, 8(12):2182, 1965.

[11] Pablo Higuera, Javier L Lara, and Inigo J Losada. Three-dimensional interaction of waves and porous coastal structures using openfoam®. part i: formulation and validation. *Coastal Engineering*, 83:243–258, 2014.

[12] Pablo Higuera, Javier L Lara, and Inigo J Losada. Three-dimensional interaction of waves and porous coastal structures using openfoam®. part ii: Application. *Coastal Engineering*, 83:259–270, 2014.

[13] C W Hirt and Billy D Nichols. Volume of fluid (vof) method for the dynamics of free boundaries. *Journal of computational physics*, 39(1):201–225, 1981.

[14] Tian-Jian Hsu, Tsutomu Sakakiyama, and Philip L-F Liu. A numerical model for wave motions and turbulence flows in front of a composite breakwater. *Coastal Engineering*, 46(1):25–50, 2002.

[15] Javier L Lara, Manuel del Jesus, and Inigo J Losada. Three-dimensional interaction of waves and porous coastal structures: Part ii: Experimental validation. *Coastal Engineering*, 64:26–46, 2012.

[16] JL Lara, N Garcia, and IJ Losada. Rans modelling applied to random wave interaction with submerged permeable structures. *Coastal Engineering*, 53(5):395–417, 2006.

[17] Inigo J Losada, Javier L Lara, Erik D Christensen, and Nicolas Garcia. Modelling of velocity and turbulence fields around and within low-crested rubble-mound breakwaters. *Coastal Engineering*, 52 (10):887–913, 2005.

[18] Hocine Oumeraci, Andreas Kortenhaus, William Allsop, Marten de Groot, R Crouch, H Vrijling, and H Voortman. *Probabilistic design tools for vertical breakwaters*. CRC Press, 2001.

[19] Suhas Patankar. *Numerical heat transfer and fluid flow*. CRC Press, 1980.

[20] DH Peregrine. Water-wave impact on walls. *Annual review of fluid mechanics*, 35(1):23–43, 2003.

[21] Y-M Scolan. Some aspects of the flip-through phenomenon: A numerical study based on the desingularized technique. *Journal of fluids and structures*, 26(6):918–953, 2010.

[22] S Takahashi, K Tanimoto, and K Shimosako. A proposal of impulsive pressure coefficient for the design of composite breakwaters. In *Proc. of the International Conference of Hydro-Technical Engineering for Port and Harbour Construction*, pages 489–504, 1994.

[23] S Takahashi, K Tanimoto, K Shimosako, et al. Dynamic response and sliding of breakwater caissons against impulsive breaking wave forces. In *Proc. Intl. Workshop" Wave Barriers in Deep Waters*, pages 362–399, 1994.